Guam Comprehensive Flood Study – Part 2

Flood Hazard Study
Umatac River

Umatac Village, Guam

Final Report
31 March 2020

Prepared by:
U.S. Army Corps of Engineers, Honolulu District

Prepared for:
Government of Guam, Bureau of Statistics and Plans

This page is intentionally blank.

Executive Summary

The Guam Comprehensive Flood Study represents a collaborative approach between the US Army Corps of Engineers (USACE) and the Government of Guam to understand flooding hazards across the island. The technical work done by USACE is meant to serve as the planning framework that the Government of Guam will use to work toward reducing flood risk for its communities.

The purpose of the study is to provide the Government of Guam with 1) an update of the regional flood frequency analysis for southern Guam; 2) site-specific hydrologic and hydraulic analysis of two to four flood prone areas within the inventory; and 3) preliminary flood mitigation design concepts for the aforementioned sites. Documentation for the study was divided into four parts:

Part 1 – Flood Frequency Estimates for Streams on Guam

Part 2 – Flood Hazard Study for Umatac River, Guam

Part 3 – Flood Hazard Study for Nelansa (Manell) River, Guam

Part 4 – Flood Hazard Study for Upper Namo River, Guam

This document presents information on Part 2, the objective of which is to 1) provide estimates of the magnitudes of the 50%, 20%, 10%, 4%, 2%, 1%, and 0.2% Annual Exceedance Probability (AEP) peak stream discharges at Umatac River, 2) provide inundation maps representing existing conditions in the floodplain for the 1% and 0.2% AEP flood events, and 3) provide site-specific preliminary flood mitigation design concepts to address flooding caused by Umatac River.

Three different methods were used to estimate the peak flow for the 8 frequency events: 1) stream gage analysis following Bulletin 17B methodology, 2) regional regression equations as introduced in Part 1 of this study, and 3) rainfall runoff modeling. The peak flow estimates computed by the rainfall-runoff model (Table 4-21) were determined to be the most reliable dataset as it was based on site-specific basin characteristics and calibrated to historical streamflow data. These flows were used as input for the hydraulic model.

A one-dimensional, steady flow model was created using the Hydrologic Engineering Center's River Analysis System (HEC-RAS) software. Field measurements and observations made during the October 2018 site visit were incorporated into the geometry of the HEC-RAS model. Modeling results indicate floodwaters enter the overbank areas and residential properties as frequently as the 50% AEP (2-yr) event due to the narrow channel, low overbanks, and structural constrictions along the river. The 1% AEP (100-yr) inundation map is presented in Appendix A.

Based on typical sediment levels observed during the October 2018 site visit, the Umatac Bridge would be able to pass the 50% AEP (2 year) flood event with marginal flooding upstream and downstream to residential properties. During the 20% AEP (5 year) event, residential properties upstream and downstream of the bridge would begin flooding a reasonable amount. The bridge itself would overtop during the 1% AEP (100 year) event.

Flood mitigation alternatives specific to this site include: 1) reforestation, 2) pre-storm cleaning, and 3) an inline weir and detention basin structure. Frequent fires in the watershed have resulted in the native ravine forest being replaced with the more resilient and fire-adapted savannah grass. Savannah grass burns easily, but the roots remain alive and soon after an area burns over it sprouts again. Although the risk of fire and resulting bare soil is higher with savannah grass, its ability to quickly recover limits the time the soil is exposed. Small trees are often killed entirely when burned. In the short term, the savannah grass may be helping to reduce overland flow and sediment runoff by providing immediate cover to otherwise bare soil. However, with each fire, the organic component of the soil is eroded and the ability for any type of vegetation to maintain its existence is lost, resulting in "badland" areas of bare soil. Even the savannah grasses would be unable to grow in these badland areas. Long term effects from burning and the creation of badlands are a real threat in terms of flood risk. The estimated cost of construction to reforest a 1 acre site is approximately $51,400 with a 43% contingency for a total estimated construction contract cost of $73,600.

Regular maintenance to remove the sediment shoals under and near the Umatac Bridge would increase the channel's ability to convey flood waters and reduce the bridge's risk of overtopping during a large storm event. When the Umatac Bridge is obstructed

approximately 50%, the bridge overtops as early as the 10% AEP (10 year) flood event according to the simulated model. When the amount of obstruction under the Umatac Bridge is decreased to approximately 20%, the bridge is unlikely to be overtopped for even the 0.2% AEP (500 year) flood event. Although the risk of overtopping is reduced in this scenario, reasonable flooding to the residential properties near the bridge still occur during the 20% AEP (5 year) event. The estimated cost of construction is $49,800 with a 26% contingency for a total estimated construction contract cost of $62,700.

An inline weir and detention basin can be effective in reducing peak flow along a river by storing excess runoff and gradually reducing it over time. As the Madog River has a peak flow that is approximately 1.5 times greater than the Laelae River, the proposed detention basin was located along the Madog River, upstream of the developed area, and at a natural constriction in the topography. Additionally, this feature has the added benefit of reducing the amount of sediment being transported to the ocean; however, it may also require regular removal of the sediment collected in the basin every 1-2 years. The estimated cost of construction for the inline weir and detention basin is approximately $920,000 with a 35% contingency for a total estimated construction contract cost of $1,245,000.

TABLE OF CONTENTS

APPENDICES

LIST OF FIGURES

LIST OF TABLES

LIST OF ACRONYMS & ABBREVIATIONS

- % – percent
- A – area; drainage area
- AEP – annual exceedance probability
- BSP – Bureau of Statistics and Plans
- CN – curve number
- D – depth; bank-full depth
- DEM – digital elevation model
- DPW – Department of Public Works
- FCP – flood control project
- FHWA – Federal Highway Administration
- FPMS – Flood Plain Management Services
- ft - feet
- GCMP – Guam Coastal Management Program
- GIS – geographical information systems
- GUVD04 – Guam Vertical Datum of 2004
- HEC – Hydrologic Engineering Center
- HMS – Hydrologic Modeling Software
- IREI – Island Research & Education Initiative
- JALBTCX – Joint Airborne Lidar Bathymetry Technical Center of Expertise
- km – kilometer
- L – length; length of flow path; length of space between cross sections
- LiDAR – Light Detection and Ranging
- m – meter
- mi – miles
- MHHW – mean higher high water
- MLLW – mean lower low water
- MSL – mean sea level
- *n* – Manning's coefficient
- NAD83 – North American Datum of 1983
- NCDC – National Climatic Data Center
- NOAA – National Oceanic and Atmospheric Administration
- NRCS – National Resources Conservation Service
- NSE – Nash-Sutcliffe model efficiency
- OCD – Office of Civil Defense
- OHS – Office of Homeland Security
- PFDS - Precipitation-Frequency Data Server
- R – storage coefficient
- RAS - River Analysis System
- S_0 = mean channel slope
- SSP – Statistical Software Package
- T_c - time of concentration
- TR-55 - Technical Release 55
- U.S. – United States

- USACE – U.S. Army Corps of Engineers
- USDA – U.S. Department of Agriculture
- USGS – U.S. Geological Survey
- UTM – Universal Transverse Mercator
- WERI – Water and Environmental Research Institute of the Western Pacific
- WGS – World Geodetic System
- W.S. – water surface
- XS - HEC-RAS cross section
- yr - year

1. Introduction

1.1 Authority

This study was completed under the authority of the Flood Plain Management Services (FPMS) Program provided by Section 206 of the 1960 Flood Control Act (Public Law 86-645). As amended, the U.S. Army Corps of Engineers (USACE) is to provide a full range of flood risk information, technical services, and planning guidance in support of active floodplain management.

1.2 Purpose and Scope

The Guam Comprehensive Flood Study represents a collaborative approach between the US Army Corps of Engineers (USACE) and the Government of Guam to understand flooding hazards across the island. The technical work done by USACE is meant to serve as the planning framework that the Government of Guam will use to work toward reducing flood risk for its communities.

The purpose of the study is to provide the Government of Guam with 1) an update of the regional flood frequency analysis for southern Guam; 2) site-specific hydrologic and hydraulic analysis of two to four flood prone areas within the inventory; and 3) preliminary flood mitigation design concepts for the aforementioned sites. Documentation for the study was divided into four parts:

Part 1 – Flood Frequency Estimates for Streams on Guam

Part 2 – Flood Hazard Study for Umatac River

Part 3 – Flood Hazard Study for Nelansa (Manell) River

Part 4 – Flood Hazard Study for Upper Namo River

This document presents information on Part 2, the objective of which is to 1) provide estimates of the magnitudes of the 50%, 20%, 10%, 4%, 2%, 1%, and 0.2% Annual Exceedance Probability (AEP) peak stream discharges at Umatac River, 2) provide inundation maps representing existing conditions in the floodplain for the 1% and 0.2% AEP flood events, and 3) provide site-specific preliminary flood mitigation design concepts to address flooding caused by Umatac River.

1.3 **Partner Agency**

The Government of Guam, Bureau of Statistics and Plans (BSP), Guam Coastal Management Program (GCMP) is designated as the proponent of the study because of their broad coordination authorities and comprehensive planning mandates. Responsible for land and natural resource planning, GCMP is often involved with issues concerning natural hazards that impact the daily lives of Guam's communities. A common issue faced by Guam residents and Government agencies is flooding. What started out as GCMP's work to provide a basic characterization of flooding problems in the village of Merizo, has now grown to a comprehensive technical assessment of major flood prone areas on the Island because of the partnership and resources provided by USACE Honolulu District.

1.4 **Site Visit**

In October 2018, USACE personnel conducted a site visit to measure bridge crossings, take photographs of the channel, and investigate the three priority sites included in the Guam Comprehensive Flood Study. They also met with BSP representatives to understand the unique challenges at each priority site and overall flood history. Several photos included in this report are from that site visit. Bridge and channel measurements were incorporated into the hydraulic model. Site-specific information provided by BSP added value to the development of alternatives for flood mitigation.

2. Watershed Description

2.1 Location

Umatac River is located in the village of Umatac, located on the southwestern coast of the United States territory of Guam. Two tributaries flow into the Umatac River upstream: the Laelae River in the north, and the Madog River in the south.

2.2 Topography

The triangular-shaped Umatac River Basin (Figure 2-1) drains a total of 5.49 square kilometers (km^2); 2.12 square miles (mi^2). It is approximately 3.39 kilometers (km); 2.10 miles (mi) wide, and 2.82 km (1.75 mi) long, extending from Mount Bolanos to Umatac Bay. The basin slope is a moderately-steep 13 percent (%), with Mount Sasalaguan approximately 371 meters (m); 1,217 feet (ft) above sea level. Steep land slopes and soils with a low permeability are often associated with greater stream incision. The longest watercourse in the basin is approximately 2.0 km (1.2 mi) with an approximate channel slope of 1.1%.

2.3 Geology

The basin of the Umatac River is geologically defined by two formations: the Facpi Formation of Eocene age and the Umatac Formation of Oligocene – late Miocene age. As the oldest exposed rock in the basin, the Facpi Formation is located at the base of the watershed and underlie all other exposed rock units (Gingerich, Hydrologic Resources of Guam, 2003). It is comprised of pillow basalts interbedded with increasing amounts of pyroclastics near the top (Stark, 1963). The Umatac Formation is composed (from oldest to youngest) of about 76.2 m (250 ft) of reef and foreef limestone (Maemong Limestone Member), about 229 m (750 ft) of tuff breccia and volcanic conglomerate (Bolanos Pyroclastic Member, Shroeder Flow Member), and about 15.2 m (50 ft) of basalt and andesite flows (Dandan Flow Member) (Gingerich, Hydrologic Resources of Guam, 2003). These rocks and the alluvial deposits in the stream valley have a low permeability.

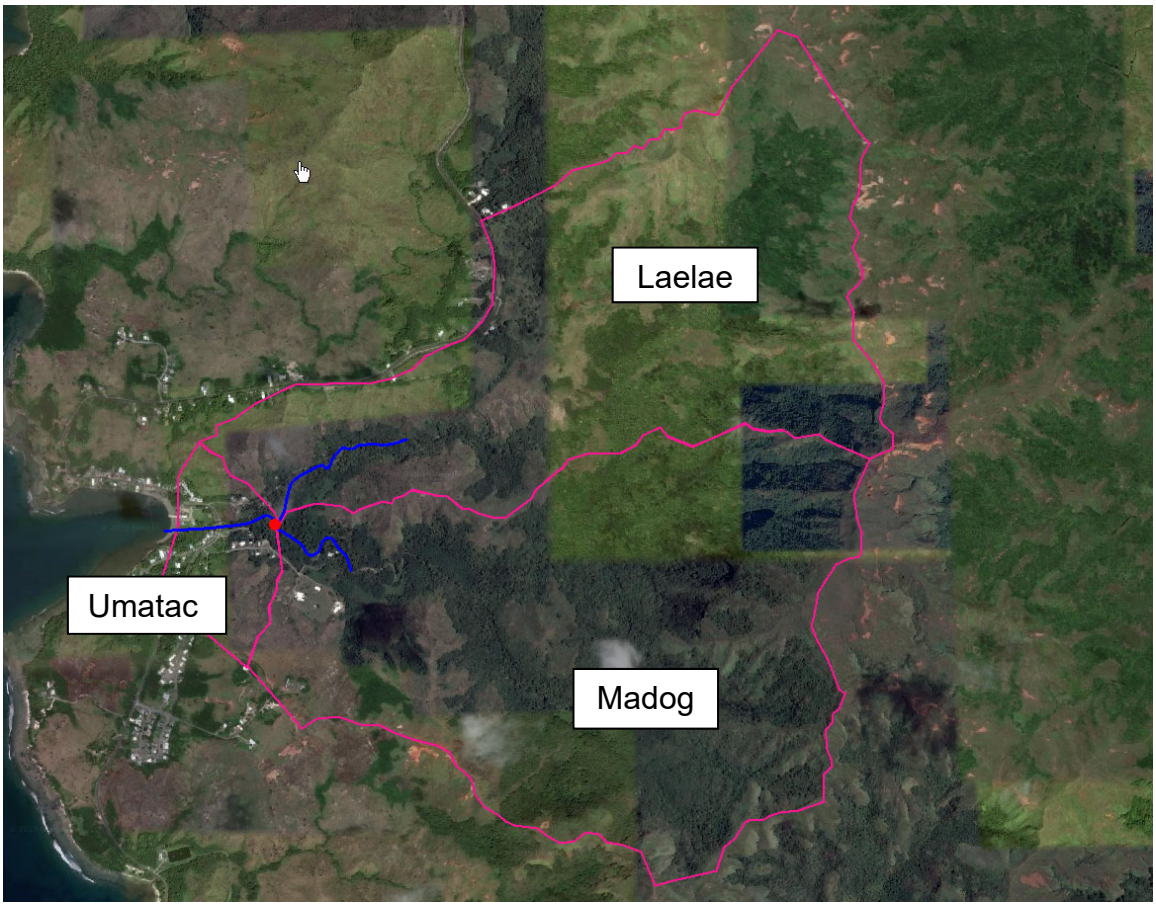

Figure 2-1: Delineated Subbasins of the Umatac River

2.4 **Soils**

Near the coast and lower elevations, the soil primarily belongs to the Inarajan series, which is a silty clay of volcanic origins. It has a slow permeability rate, seasonal high water table, and is typically a dark gray color. Erosion is not a problem for this soil type (University of Guam, 2016).

In the volcanic uplands, the soil primarily belongs to the Akina and Agfayan series (Soil Conservation Service, 1985). These soils are classified as silty clay, volcanic in origin. The soils have moderately slow permeability, resulting in rapid runoff. Erosion is a serious concern for Akina soils, which are characteristically dark reddish brown to dark red in color compared to the Agfayan soils which are black, yellow, or brown (University of Guam, 2016). Akina soil is also found along the valley bottoms and riverbeds in the lower Umatac watershed, along with soil belonging to the Togcha and Ylig series. These soils have similar characteristics to Akina.

2.5 **Vegetation**

Within the study area, a heavy growth of tropical vegetation borders the inland areas of rivers and represents a plant community known as the ravine forest. Sharp divisions between the non-native savannah grasslands and ravine forest provide particularly aesthetic contrasts in the study area. Fires occur frequently and are often intentionally set by people to draw deer and pigs out when hunting, to clear fields for farming, or as wildfire arson. The spatial extent of the savannah grasslands has increased in size as the fire-adapted grasslands quickly replace the burned forest edge. The southern uplands are some of the island's only expanses of unspoiled terrain.

2.6 **Climate**

Guam's climate is tropical marine, reflecting the nearness of the equator and the influence of warm surrounding waters. Wind and rainfall are the most variable elements; humidity, temperature and pressure remain fairly constant. The year is divided into a wet (July through December) and a dry (January through June) season with pronounced differences in rainfall.

Two principal kinds of storms contribute to the climatic character of Guam: small-scale storms, consisting of thunderstorms and squalls, and large systems of tropical storms and typhoons. The small-scale disturbances may dominate an area of only a few square miles. Larger cyclonic storm systems may dominate an area as large as 300,000 square miles and can persist for a week or more.

Major tropical cyclonic disturbances of these kinds occur in all months, but they are prevalent during the rainy season with the greatest probability in the months of October and November. These typhoons are actually tropical storms accompanied by winds of 65 knots (120 kilometers per hour) or greater. Based on the information provided by the Digital Atlas of Southern Guam website, "an average of three tropical storms and one typhoon pass within 180 nautical miles (330 km) of Guam each year" with the most intense typhoon to pass over Guam recently being Super Typhoon Pongsona on December 8, 2002 (WERI and IREI, n.d.).

2.6.1 **El Niño Years**

The term *El Niño* refers to a periodic warming (every two to seven years) of the Pacific Ocean surface waters. These conditions often result in tropical rains shifting eastward across the Pacific and an increased risk of typhoons from March through July and October through December. Rainfall is characteristically greater at the start of El Niño conditions (beginning in May or June), near normal by December, and well below average by the following February. (NOAA Pacific RISA 2015). The duration, strength, and impacts of El Niño events vary, but three periods are universally accepted as having produced very strong conditions: 1982-83, 1997-98, and 2015-16 (NOAA Climate Prediction Center 2018).

3. Geographic Information Systems Data

Several terrain models and data layers were used to perform the hydrologic and hydraulic analysis of the study area. The Geographical Information Systems (GIS) data, sources, and description are summarized in the following sections.

3.1.1 **Datum and Projection**

The datum and projection for this study is as follows:

Horizontal projection: Universal Transverse Mercator (UTM) Zone 55 North (N), meters

Horizontal datum: World Geodetic System 1984 (WGS84)

Vertical Datum: Guam Vertical Datum of 2004 (GUVD04)

Tidal Epoch: 1983 – 2001

3.1.2 **Elevation**

The following sources of elevation data were used in this study:

Table 3-1: Elevation Data Type and Sources

Survey year	Agency	Data type	Location
2012 – 2013	USGS	LiDAR	Island of Guam
2007	JALBTCX	LiDAR	Island of Guam

Light Detection and Ranging (LiDAR) data were collected across the island of Guam by NOAA Office for Coastal Management (OCM) in 2012 and 2013 for the U.S. Geological Survey (USGS). The data is in North Atlantic Datum 1983 (NAD83) MA11, vertically referenced to GUVD04, has a vertical accuracy of +/- 8 centimeters (cm), and horizontal accuracy of +/- 0.11 m. This data was given first priority in creating the merged digital elevation model (DEM) for use in this study.

LiDAR data were also collected by USACE and the Joint Airborne LiDAR Bathymetry Technical Center of Expertise (JALBTCX) in 2007 for the Government of Guam. This data includes hydrographic and topographic data depicting the elevations above and below the immediate coastal water. The topographic lidar data are vertically referenced to Mean Sea Level (MSL) and the bathymetric lidar data are referenced to Mean Lower Low Water (MLLW). The data set has a horizontal accuracy of +/- 0.75 m and a vertical accuracy of

+/- 20 cm. The data was collected so that the horizontal and vertical datum could be specified by the user. For this project, the selected projection was the Universal Transverse Mercator (UTM) coordinate system, zone 55N. Horizontal coordinates reference the NAD83 in meters. The vertical control datum is the Guam Vertical Datum of 2004 (GUVD04), in meters.

3.1.3 **Imagery**

High resolution imagery used for background mapping of the study area is from the National Geospatial-Intelligence Agency and the USGS. World Imagery, provided by Esri, was used for larger scale background mapping, such as when it was necessary to show the entire island of Guam.

3.1.4 **Digital Atlases of Guam**

The Digital Atlas of Southern Guam and the Digital Atlas of Northern Guam, by WERI and IREI, provide public access to geospatial data that covers the entire island of Guam. The website address is: http://south.hydroguam.net/ and http://north.hydroguam.net/. Several files were downloaded and used as a resource for this study, including files on geology, climate, soil, surface water, land cover, and infrastructure.

4. Hydrologic Analysis

Methods for estimating the peak flow for the 50%, 20%, 10%, 4%, 2%, 1%, 0.4%, and 0.2% AEP (2-, 5-, 10-, 25-, 50-, 100-, 250-, and 500-year) flood events (8 profiles) include the following:

1. Stream Gage Analysis
2. Regional Regression Equations
3. Rainfall-Runoff Modeling

Other peak flow estimates previously published (for reference):

1. 2007 FEMA FIS

4.1 Stream Gage Analysis

There is one streamflow gaging station located within the Umatac River basin: *16816000 Umatac River at Umatac, Guam* (USGS 6000). This gaging station is no longer operated and maintained by the U.S. Geological Survey (USGS), but provides annual peak flow record data for 33 events. In the adjacent watershed, the USGS continues to operate and maintain a streamflow gaging station that provides both instantaneous and peak flow data: *16809600 La Sa Fua River near Umatac, Guam* (USGS 9600) with 32 annual events.

4.1.1 Bulletin 17B

Annual peak flow data from USGS 6000 and USGS 96000 were analyzed individually using methodology from Bulletin 17B (USGS. Office of Water Data Coordination 1982) as applied by the Hydrologic Engineering Center's Statistical Software Package (HEC-SSP) program (version 2.2, HEC, 2019) which follows the Bulletin 17B guidance. The weighted skew option was used, which weights the computed station skew with the generalized regional skew. A generalized skew value of 0.220 and mean-square error of 0.169 was adopted as determined in Part 1 – Flood Frequency Estimates for Streams on Guam.

Table 4-1: Peak Flow Data from Gaged Data by Bulletin 17B Analysis in HEC-SSP

Location	Peak Flow (m^3/s)[1]							
	2-yr (50%)	**5-yr (20%)**	**10-yr (10%)**	**25-yr (4%)**	**50-yr (2%)**	**100-yr (1%)**	**250-yr (0.4%)**	**500-yr (0.2%)**
USGS 6000	75.5	118	151	198	237	279	342	393
USGS 9600	29.4	40.5	47.8	57.2	64.3	71.0	80.9	88.2
[1]: rounded to three significant figures								

4.2 **Regional Regression Equations**

In Part 1 of this study, regional regression equations were developed for estimating various peak flow magnitudes at ungaged, unregulated sites in southern Guam. These equations were used to estimate peak flow at USGS 6000 and USGS 9600 to show how the different methodologies compare. The results are presented in Table 4-2. Overall, the difference is within an acceptable range of tolerance.

Table 4-2: Peak Flow Data from Regional Regression Equations

Location	Peak Flow (m^3/s)[1]							
	2-yr (50%)	**5-yr (20%)**	**10-yr (10%)**	**25-yr (4%)**	**50-yr (2%)**	**100-yr (1%)**	**250-yr (0.4%)**	**500-yr (0.2%)**
USGS 6000	27.7	29.0	60.4	76.2	102	120	137	165
USGS 9600	21.8	22.6	46.9	58.7	78.2	90.7	103	123
[1]: rounded to three significant figures								

4.3 **Rainfall-Runoff Modeling**

Hydrologic models were created using the Hydrologic Engineering Center's Hydrologic Modeling System (HEC-HMS) software (version 4.2, HEC, 2016). This section describes rainfall, riverine, and basin characteristics that were used to create the models, as well as the resulting flow estimates for different probability events.

Two HEC-HMS models were created: one for the Umatac River basin and one for the La Sa Fua River basin. The La Sa Fua basin is adjacent to the Umatac basin and has historical streamflow data that can be used to calibrate both models. Information on both models is provided in this section.

4.3.1 **River Delineation**

Two rivers meet to form the Umatac River: the Laelae River in the north and the Madog River in the south. These rivers, and the La Sa Fua River, were delineated in GIS, extending from the upper watershed to the ocean outlet. All of the rivers are natural and unlined. Typical channel characteristics are provided in Table 4-3. Photographs showing typical conditions as observed during the October 2018 site visit are presented in Photo 4-1 through Photo 4-5.

Table 4-3: Channel Characteristics

River	Length (m) [1]	Slope (m/m) [1]	Manning's *n* [1,2]	Bottom Width (m) [2]	Side Slopes (xH:1V) [2]
Laelae	1,180	0.014	0.04	9.0	0.5
Madog	1,520	0.014	0.04	9.0	0.5
Umatac	470	0.005	0.04	10.0	0.5
La Sa Fua	3,560	0.021	0.04	8.0	0.5

Photo 4-1: Laelae River, Typical Channel Conditions

Photo 4-2: Madog River, Typical Channel Conditions

Photo 4-3: Umatac River, Between Upstream Confluence and Umatac Bridge

Photo 4-4: Umatac River, Looking Downstream from Umatac Bridge to Bay Outlet

Photo 4-5: Umatac River, Looking Toward Bay Outlet

4.3.2 **Subbasin Delineation**

The corresponding drainage areas that contribute flow to the Laelae River, Madog River, Umatac River, and La Sa Fua River, were also delineated in GIS. They are respectively referred to as “Laelae_DA,” “Madog_DA,” “Umatac_DA,” and “LaSaFua_DA” in the HEC-HMS model and this report. The layout for the two basin models created in HEC-HMS are shown in Figure 4-1 and Figure 4-2. Table 4-4 identifies the total drainage area and centroid coordinates for each subbasin.

Table 4-4: Basin Characteristics

HEC-HMS Subbasin Name	Area (km2)	Centroid	
		Latitude	Longitude
Laelae_DA	2.39	13.306	144.679
Madog_DA	2.84	13.294	144.678
Umatac_DA	0.261	13.297	144.665
LaSaFua_DA	2.73	13.315	144.674

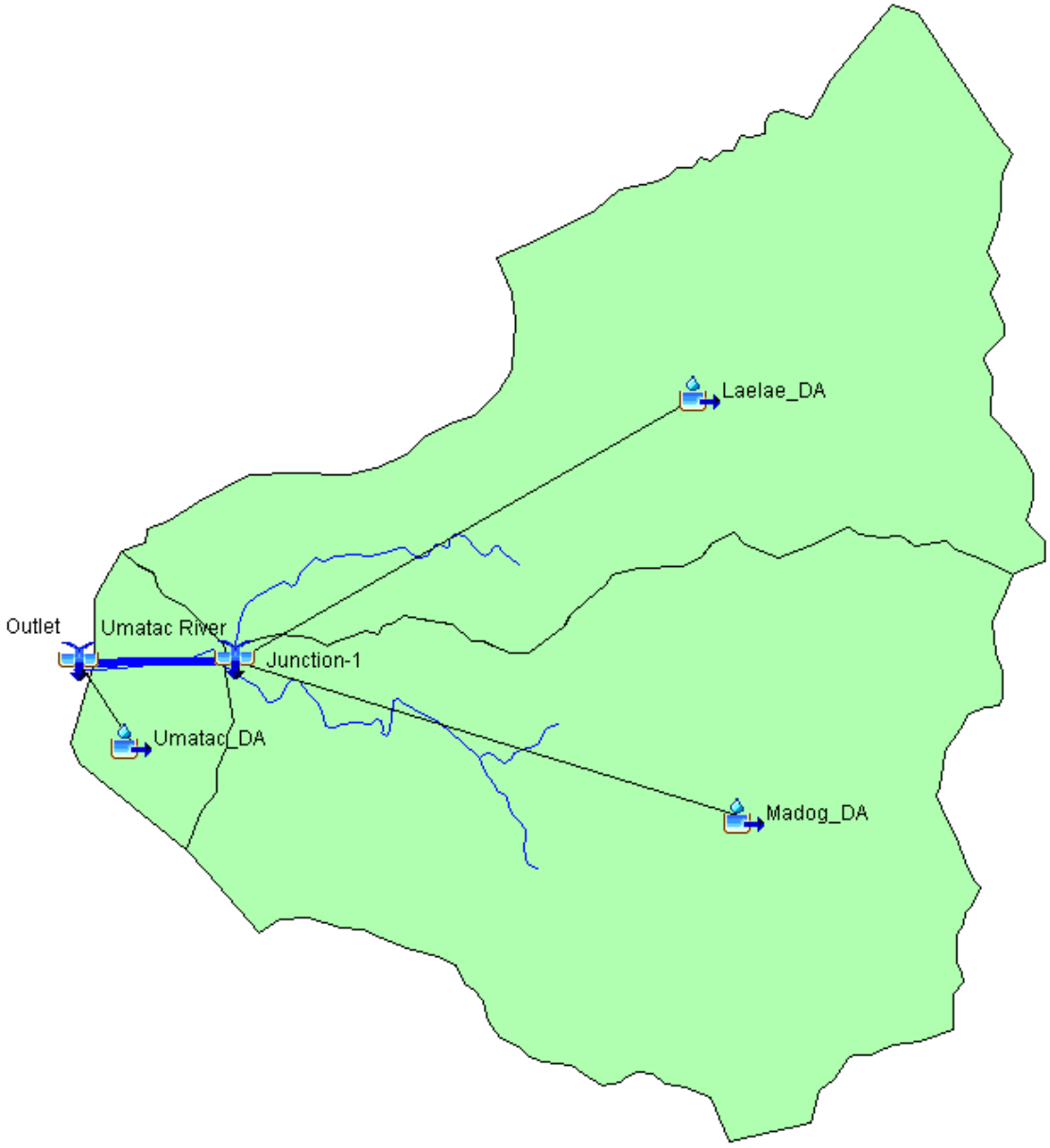

Figure 4-1: HEC-HMS Basin Model, Umatac River Basin

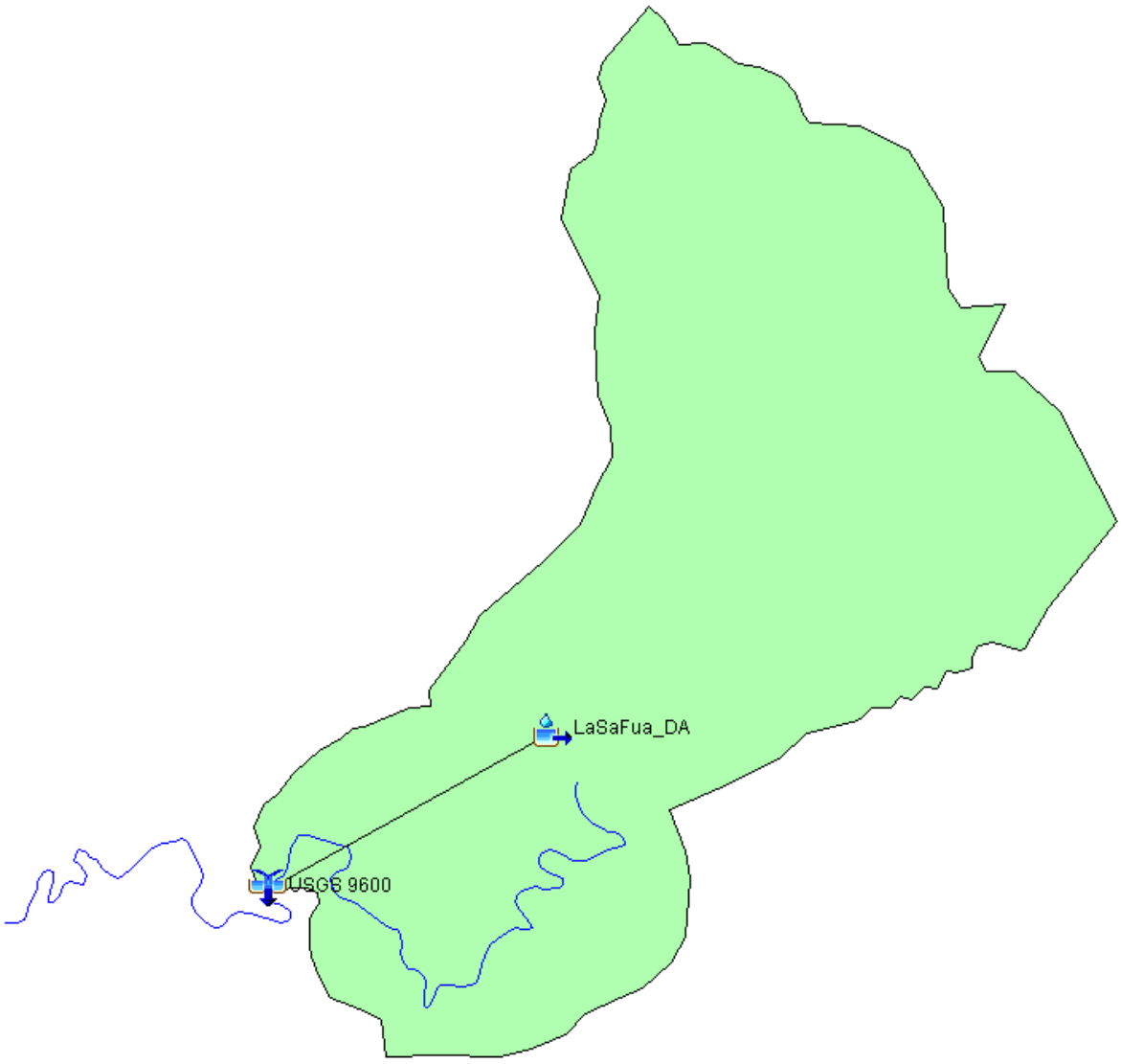

Figure 4-2: HEC-HMS Basin Model, La Sa Fua River Basin

4.3.3 **Subbasin Loss Parameterization**

As described in Section 2.3, Geology, the low-permeability volcanic rocks and alluvial deposits along the streambed slow the infiltration of rainwater. Initial loss was set to 0.1 millimeters (mm), the lowest value accepted by the HEC-HMS program. Constant loss was estimated to be 0.15 mm per hour (hr). The percent impervious was approximated in GIS to be between 0.25% and 5% (see Table 4-5).

Table 4-5: Subbasin Loss Parameters

HEC-HMS Subbasin Name	Initial Loss (mm)	Constant Rate (mm/hr)	Impervious (%)
Laelae_DA	0.1	0.15	0.25
Madog_DA	0.1	0.15	0.25
Umatac_DA	0.1	0.15	5
LaSaFua_DA	0.1	0.15	0.5

4.3.4 **Subbasin Transform Parameterization**

The excess precipitation in each subbasin was transformed into surface runoff by applying the Clark Unit Hydrograph method in the hydrologic model. This method requires two input parameters for each subbasin: the time of concentration (T_c) and the storage coefficient (R). The time of concentration, or the time it takes for runoff to travel from the most distant point in the watershed to the outlet, was calculated in accordance to the TR-55 manual's guidance. The TR-55 method breaks the surface flow in the watershed into three flow regimes (NRCS, Conservation Engineering Division, 1986). As water travels along the longest flow path in the subbasin, it is transformed from sheet flow (Table 4-6) to shallow concentrated flow (Table 4-7) to open channel flow (Table 4-8).

A time value is calculated for each flow regime. The time of concentration of a watershed is calculated by summing the travel time of flow through each of these flow regimes. GIS was used to determine the longest flow path, slope, and flow length of each subbasin. Representative channel cross-sections were estimated from the LiDAR data or measured in the field. Additional data required for the TR-55 method, such as the 2-year, 24-hour rainfall, were entered based on published data from National Oceanic and Atmospheric Administration (NOAA)'s Atlas 14 Precipitation-Frequency Data Server (PFDS) for the centroid locations listed in Table 4-4. The computed times of concentration are presented in Table 4-9.

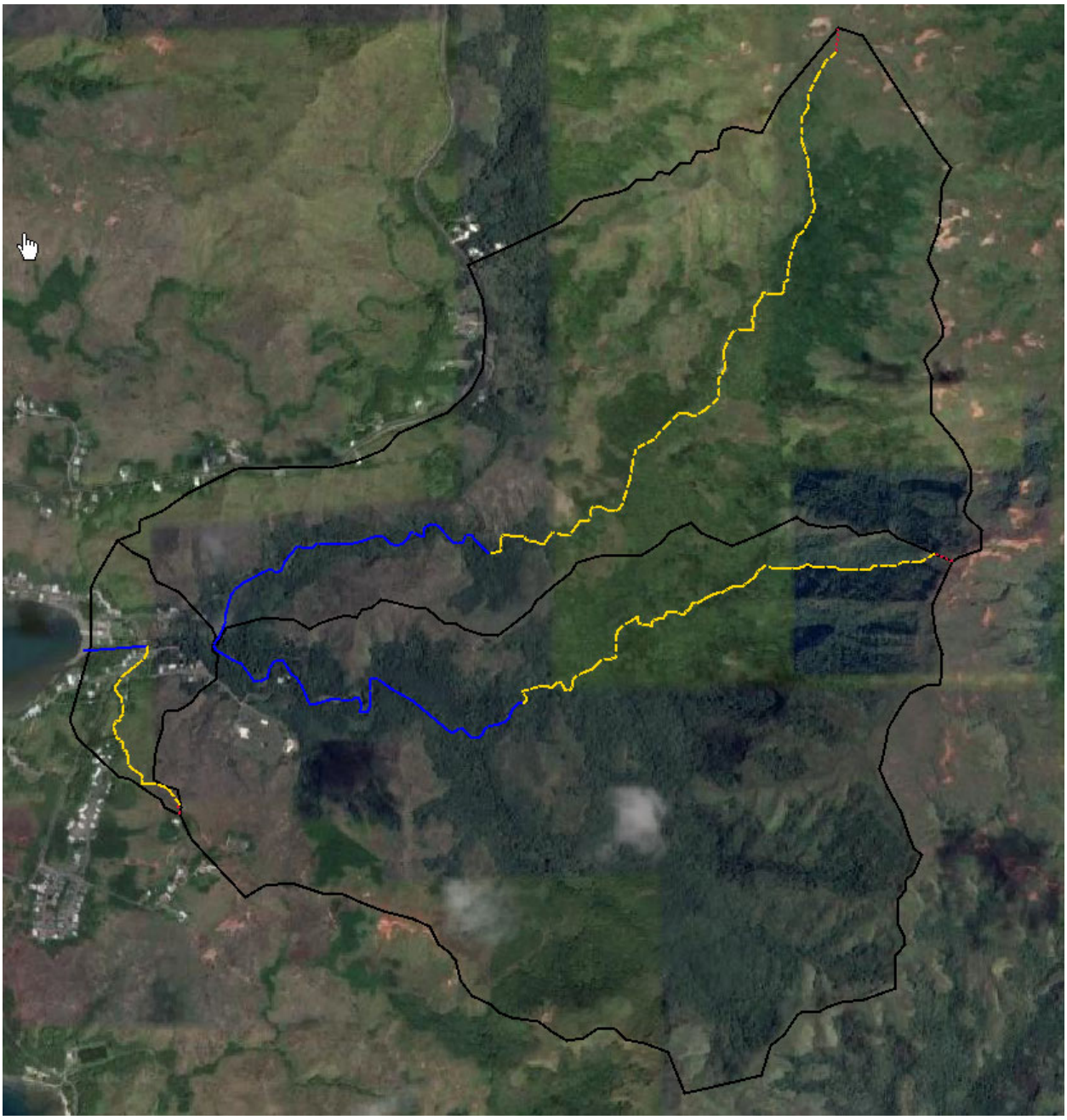

Figure 4-3: Sheet Flow, Shallow Concentrated Flow, and Channel Flow Delineated, Umatac River Basin

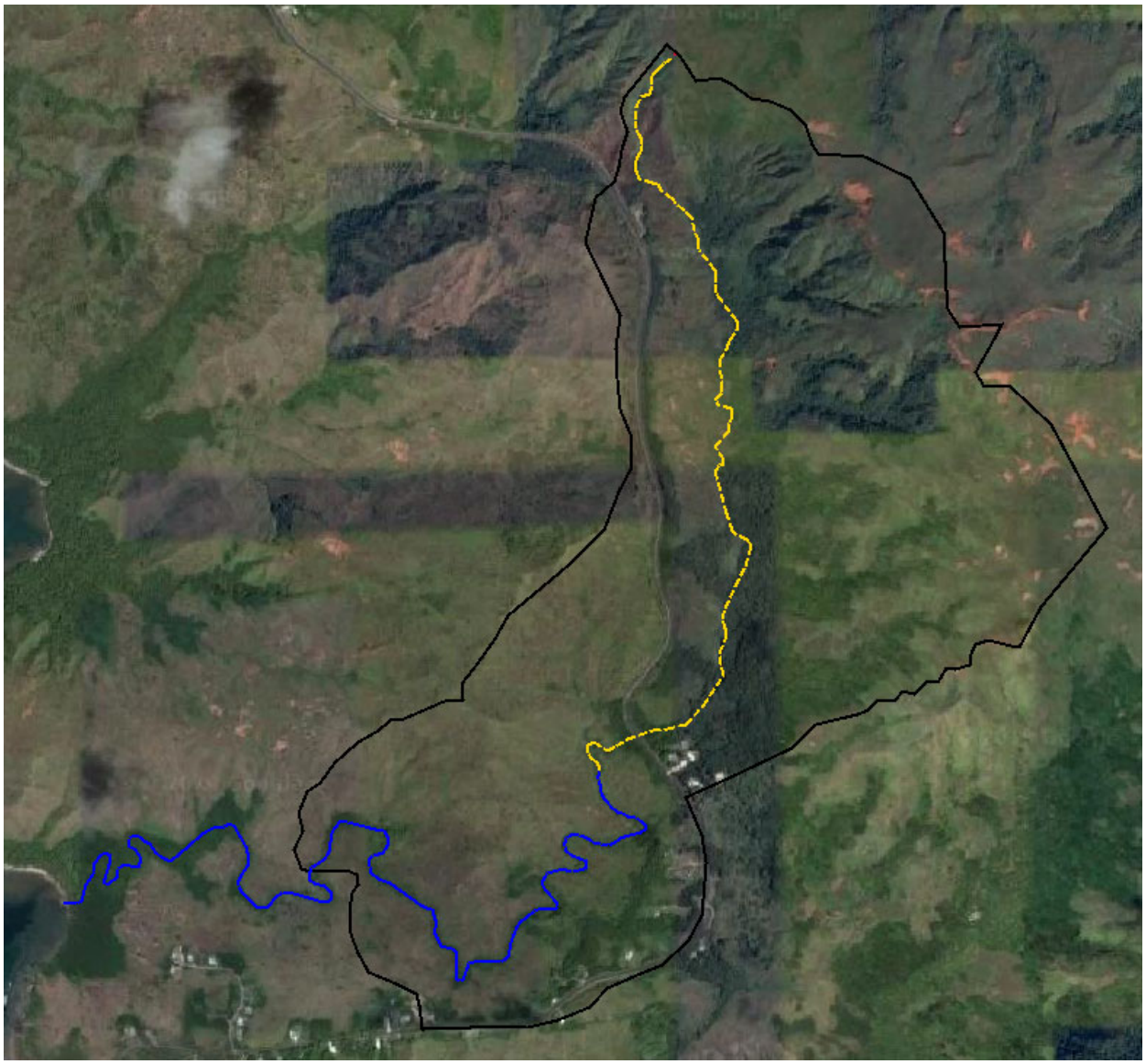

Figure 4-4: Sheet Flow, Shallow Concentrated Flow, and Channel Flow Delineated, La Sa Fua River Basin

Table 4-6: Sheet Flow Characteristics for each Subbasin

HEC-HMS Subbasin Name	Manning's *n*	Sheet Flow Length (m)	Land Slope (m/m)	2-yr, 24-hr Rainfall (mm)	Tc, sheet (hrs)
Laelae_DA	0.4	76.6	0.094	172	0.277
Madog_DA	0.4	58.6	0.420	165	0.125
Umatac_DA	0.4	27.9	0.358	164	0.074
LaSaFua_DA	0.4	15.5	0.588	175	0.037

Table 4-7: Shallow Concentrated Flow Characteristics for each Subbasin

HEC-HMS Subbasin Name	Surface Description	Shallow Flow Length (m)	Watercourse Slope (m/m)	Average Velocity (m/s)	Tc, shallow (hrs)
Laelae_DA	Unpaved	2,380	0.139	1.83	0.361
Madog_DA	Unpaved	1,650	0.190	2.13	0.215
Umatac_DA	Unpaved	686	0.128	1.75	0.109
LaSaFua_DA	Unpaved	2,580	0.101	1.57	0.456

Table 4-8: Channel Flow Characteristics for each Subbasin

HEC-HMS Subbasin Name	Hydraulic Radius (m)	Channel Slope (m/m)	Manning's *n* Channel	Velocity (m/s)	Flow Length (m)	Tc, channel (hrs)
Laelae_DA	0.845	0.014	0.04	28.5	1,180	0.124
Madog_DA	0.845	0.015	0.04	29.5	1,400	0.142
Umatac_DA	0.858	0.002	0.04	10.9	204	0.056
LaSaFua_DA	0.830	0.021	0.04	34.5	2,080	0.180

Table 4-9: Initial Time of Concentration for each Subbasin

HEC-HMS Subbasin Name	Time of Concentration, Tc (hrs)
Laelae_DA	0.762
Madog_DA	0.482
Umatac_DA	0.239
LaSaFua_DA	0.673

The Clark Unit Hydrograph storage coefficient, R, accounts for storage in the watershed. This parameter was determined using a mathematical relationship between the longest flow path, drainage area, and time of concentration. An equation was adopted from the "Drainage Design Manual for Maricopa County" (Flood Control District of Maricopa County, 2013) for use in this study. This relationship was used to make an initial estimate of the storage coefficient of each sub-basin. These estimates were adjusted during the hydrologic model calibration. The equation used is as follows:

$$R = 0.37{T_c}^{1.11}A^{-0.57}L^{0.80}$$

R: Storage Coefficient

Tc: Time of Concentration (hrs)

A: Drainage Area (square miles)

L: Length of flow path (miles)

The initial values for the storage coefficient parameter are summarized in Table 4-10.

Table 4-10: Initial Storage Coefficients for each Subbasin

HEC-HMS Subbasin Name	Time of Concentration (hrs)	Area (mi^2)	Length of Flow (mi)	Storage Coefficient, R
Laelae_DA	0.762	0.923	2.26	0.550
Madog_DA	0.482	1.10	1.93	0.264
Umatac_DA	0.239	0.101	0.570	0.178
LaSaFua_DA	0.673	1.05	2.91	0.545

4.3.5 **Subbasin Baseflow**

There is little baseflow, based on observations made during the 2018 site visit and review of historical streamflow data. Baseflow was not included in the HEC-HMS models.

4.3.6 **Model Calibration**

The rainfall-runoff model was calibrated using instantaneous rainfall data provided by USGS 131729144393766 (USGS 3766) for the period of October 2007 to March 2019. This rain gage is located near the coast at Umatac, Guam. As the topography of Guam has little effect on rainfall during major precipitation events, rainfall is expected to be similar near the coast and in the upper watershed. Due to the close proximity of USGS 3766 to the La Sa Fua and Umatac watersheds, use of other rainfall gages is not necessary for calibration. Hourly rainfall data at this rain gage was also available for the July 2002, Typhoon Chata'an event. In one instance, a synthetic hyetograph was created for a calibration event (Typhoon Pongsona in December 2002) using the total rainfall midnight-to-midnight record as provided by the National Weather Service (2003) and creating a similar distribution to Typhoon Chata'an. However, this methodology is not ideal and this event was not weighted strongly in determining the final parameters.

The period of record for the Umatac streamflow gaging station, USGS 6000, is very limited: October 2007 to September 2009. As such, the La Sa Fua watershed was also modeled in HMS and calibrated to a wider range of historical events. The streamflow gage on the La Sa Fua River, USGS 16809600 (USGS 9600), provides historical observations from June 2000 to September 2018. Two events were selected for calibration purposes at Umatac: November 2007 and August 2009; and six events were selected for calibration purposes at La Sa Fua: July 2002, December 2002, August 2009, December 2009, July 2012, and September 2015.Table 4-11 and Table 4-12 present the effectiveness of calibration efforts to match the historical peak flow and hydrograph for each event. The Nash-Sutcliffe model efficiency (NSE) coefficient is used to assess the predictive power of hydrologic models. This number can range from -∞ to 1. An efficiency of 1 corresponds to a perfect match of the simulated discharge to observed data (Moriasi, et al., 2007). Generally a model is sufficiently calibrated if the NSE is at least 0.6. Calibration of peak flow (Column D) was prioritized over hydrograph shape (Column E) for each event.

Table 4-11: Observed and Computed Peak Flows for the Umatac Watershed

A	B	C	D	E
Calibration Event	**Observed Peak Flow (m3/s)**	**Computed Peak Flow (m3/s)**	**Percent Difference (%)**	**Nash-Sutcliffe**
Nov 2007	74.5	74.5	0	0.713
Aug 2009	90.9	89.2	1.89	0.822

Table 4-12: Original and Calibrated Peak Flows for the La Sa Fua Watershed

A	B	C	D	E
Calibration Event	**Observed Peak Flow (m3/s)**	**Computed Peak Flow (m3/s)**	**Percent Difference (%)**	**Nash-Sutcliffe**
Jul 2002	60.6	60.3	0.496	0.614
Dec 2002	28.6	28.7	0.350	0.219
Aug 2009	28.1	28.7	2.11	0.680
Dec 2009	40.5	40.7	0.493	0.657
Jul 2012	43.6	43.6	0	0.117 0.804[1]
Sep 2015	45.6	16.8	92.3	0.255
Aug 2018	41.9	42.0	0.238	0.778
Sep 2018	32.3	32.3	0	0.688
[1]: rainfall data adjusted for a 30-minute delay; refer to Appendix B				

Detailed information on the calibration of specific events is provided in Appendix B. Each calibration scenario was assigned a weight of influence from zero to five (0-5), with zero having no influence, on the final HMS parameters. This value was assigned based on engineering judgment with consideration towards the ability of the calibrated model to simulate the observed peak flow and shape of the hydrograph, significance of the storm event, and other special considerations described in the preceding sections. The assigned weights of influence and the final HMS parameters for the La Sa Fua watershed are presented in Table 4-13.

Table 4-13: Initial and Final Parameters for the La Sa Fua Watershed, "LaSaFua_DA" Subbasin

Calibration Scenario	Initial Loss (mm)	Constant Loss Rate (mm/hr)	Time of Concentration (hr)	Storage Coefficient (hr)	Weight of Influence
Initial	0.1	0.15	0.673	0.545	--
Jul 2002	10	3	0.8	0.6	5
Dec 2002	15	5	0.1	2	1
Aug 2009	40	15	0.5	0.65	3
Dec 2009	20	13	0.1	0.4	3
Jul 2012	25	0.1	0.28	0.1	2
Sep 2015	10	3	1	0.1	0
Aug 2018	30	3	0.34	0.3	3
Sep 2018	45	1	0.3	0.3	3
Final	**26**	**5.81**	**0.419**	**0.508**	**--**
Percent change (%)	259	37.7	-0.377	-0.069	--

Determination of the final HMS parameters for the Umatac watershed was a little trickier as it relied upon calibration scenarios from both the Umatac and La Sa Fua watersheds. Both sites simulated the August 2009, which can be used to compare differences between the two watersheds. Overall, the percent change for constant loss rate and time of concentration from their initial values were similar for both sites; a greater initial loss was used at La Sa Fua watershed; and the storage coefficient decreased for the Umatac watershed (in La Sa Fua, it increased).

Table 4-14: Initial and Final Parameters for the Umatac Watershed, "Laelae_DA" Subbasin

Calibration Scenario	Initial Loss (mm)	Constant Loss Rate (mm/hr)	Time of Concentration (hr)	Storage Coefficient (hr)	Weight of Influence
Initial	0.1	0.15	0.762	0.550	--
Nov 2007	3	1	0.7	0.18	3

Aug 2009	11	15	0.6	0.25	3
La Sa Fua[1]	25.9	5.81	0.474	0.512	5
Final	**12.7**	**3.53**	**0.585**	**0.490**	**--**
Percent Change (%)	126	22.5	-0.233	-0.109	--
[1]: Percent change from Table 4-13 of the Initial Values of Laelae_DA					

Table 4-15: Initial and Final Parameters for the Umatac Watershed, "Madog_DA" Subbasin

Calibration Scenario	Initial Loss (mm)	Constant Loss Rate (mm/hr)	Time of Concentration (hr)	Storage Coefficient (hr)	Weight of Influence
Initial	0.1	0.15	0.482	0.264	--
Nov 2007	3	1	0.75	0.12	3
Aug 2009	0.1	15	0.6	0.25	3
La Sa Fua[1]	25.9	5.81	0.300	0.246	5
Final	**10.9**	**3.24**	**0.531**	**0.208**	**--**
Percent Change (%)	108	20.6	0.101	-0.211	--
[1]: Percent change from Table 4-13 of the Initial Values of Laelae_DA					

Table 4-16: Initial and Final Parameters for the Umatac Watershed, "Umatac_DA" Subbasin

Calibration Scenario	Initial Loss (mm)	Constant Loss Rate (mm/hr)	Time of Concentration (hr)	Storage Coefficient (hr)	Weight of Influence
Initial	0.1	0.15	0.239	0.178	--
Final	**28.3**	**3.38**	**0.223**	**0.222**	**--**
Percent change (%)	117	21.5	-0.066	-0.160	--

4.3.7 **Rainfall Frequency Data**

Point precipitation frequency data were taken from the NOAA's Atlas 14 Precipitation-Frequency Data Server (PFDS) (National Weather Service, 2017). This source presents rainfall frequencies from recurrence intervals of 1 to 500 years (100% to 0.2% chance exceedance) for sites in Guam. The location points used to extract PFDS data were the approximate centroid locations for each subbasin. The latitude and longitude for these centroids are included in Table 4-4. Individual curves were used to represent each subbasins in the HEC-HMS model (see Table 4-17 through Table 4-20).

Table 4-17: Point Precipitation Frequency Estimates (in mm), Laelae_DA Subbasin

Duration	Average recurrence interval (years)							
	2	**5**	**10**	**25**	**50**	**100**	**200**	**500**
5 Minutes	16.1	19.3	21.8	25.3	27.9	30.7	33.8	37.6
15 Minutes	32.3	38.6	43.7	50.5	56.1	61.7	67.3	75.4
1 Hour	64.3	77.2	87.4	101	112	123	135	151
2 Hours	82.0	98.6	112	130	144	158	173	194
3 Hours	95.8	116	132	154	171	188	207	232
6 Hours	118	148	171	203	228	253	279	318
12 Hours	139	182	215	262	297	335	373	427
1 Day	172	226	269	328	373	419	470	536

Table 4-18: Point Precipitation Frequency Estimates (in mm), Madog_DA Subbasin

Duration	Average recurrence interval (years)							
	2	5	10	25	50	100	200	500
5 Minutes	15.5	18.7	21.2	24.7	27.4	30.2	33.0	37.1
15 Minutes	31.0	37.3	42.4	49.3	54.9	60.5	66.3	74.2
1 Hour	61.7	74.7	84.8	98.8	109	121	132	148
2 Hours	78.7	95.5	108	126	141	155	170	191
3 Hours	92.0	112	128	150	167	185	203	228
6 Hours	114	143	166	198	223	249	274	312
12 Hours	134	177	210	257	292	330	368	422
1 Day	165	219	262	320	366	414	462	528

Table 4-19: Point Precipitation Frequency Estimates (in mm), Umatac_DA Subbasin

Duration	Average recurrence interval (years)							
	2	5	10	25	50	100	200	500
5 Minutes	15.3	18.5	21.1	24.5	27.2	30.0	33.0	36.8
15 Minutes	30.7	37.1	42.1	49.0	54.6	60.2	65.8	73.9
1 Hour	61.2	74.1	84.3	98.0	109	120	132	148
2 Hours	78.0	94.7	108	126	140	154	169	190
3 Hours	91.1	111	127	149	166	184	202	227
6 Hours	113	142	165	197	222	248	274	310
12 Hours	132	175	209	254	292	328	368	419
1 Day	164	218	259	318	366	411	460	528

Table 4-20: Point Precipitation Frequency Estimates (in mm), LaSaFua_DA Subbasin

Duration	Average recurrence interval (years)							
	2	5	10	25	50	100	200	500
5 Minutes	16.4	19.6	22.1	25.7	28.5	31.2	34.0	38.1
15 Minutes	32.8	39.4	44.5	51.3	56.6	62.2	68.1	76.2
1 Hour	65.5	78.5	88.6	103	113	125	136	152
2 Hours	83.6	100	114	131	146	160	175	196
3 Hours	97.8	118	134	156	173	190	209	233
6 Hours	121	150	173	205	230	257	282	320
12 Hours	142	185	218	264	300	338	376	429
1 Day	175	230	272	330	376	424	472	538

4.3.8 **Hydrologic Model Results**

The calibrated HEC-HMS model was used to simulate the 50-, 20-, 10-, 4-, 2-, 1-, and 0.2% AEP flood frequency events. The resulting peak discharges for each subbasin are presented in Table 4-21.

Table 4-21: Calibrated Peak Flow Data from HEC-HMS for the Umatac River Basin

HEC-HMS Element Name	Drainage Area (km^2)	Peak Flow (m^3/s)[1]						
		2-yr (50%)	5-yr (20%)	10-yr (10%)	25-yr (4%)	50-yr (2%)	100-yr (1%)	500-yr (0.2%)
Laelae_DA	2.39	11.4	45.5	51.8	60.4	67.2	74.1	91.4
Madog_DA	2.84	58.7	71.5	81.5	95.3	106	117	144
USGS 6000	5.23	68.9	116	132.1	154	171	190	234
Umatac_DA	0.261	5.40	6.60	7.5	8.80	9.80	10.9	13.4
Outlet	5.49	65.5	113	130	151	166	185	226
[1]: rounded to three significant figures								

Table 4-22: Peak Flow Data from HEC-HMS for the La Sa Fua River Basin

HEC-HMS Element Name	Drainage Area (km^2)	Peak Flow (m^3/s)[1]						
		2-yr (50%)	5-yr (20%)	10-yr (10%)	25-yr (4%)	50-yr (2%)	100-yr (1%)	500-yr (0.2%)
LaSaFua_DA	2.73	43.6	53.2	60.7	71.1	78.8	87.4	107.6
USGS 9600	2.73	43.6	53.2	60.7	71.1	78.8	87.4	107.6
[1]: rounded to three significant figures								

4.4 **Reference Flows**

4.4.1 **2007 FIS**

In September 2007, the Federal Emergency Management Agency (FEMA) published Flood Insurance Study (FIS) 660001CV000A for the Territory of Guam (FEMA, 2007). This study includes peak flow estimates for Umatac River at the mouth (Table 4-23).

Table 4-23: Peak flow data from the 2007 FIS by FEMA

Location	Drainage area (km^2)	Peak flow (m^3/s)[1]			
		1/10	1/50	1/100	1/500
Mouth	5.46	93.4	136	156	204
[1]: rounded to three significant figures					

4.5 **Adopted Flows**

As the Umatac and La Sa Fua HMS models used site-specific information and was calibrated to historical data, these peak flows are the most reliable and should be used as the flow input for the hydraulic model (Table 4-22). For comparison, all three methods of estimating the peak flow at the two gage sites are presented as Figure 4-5 and Figure 4-6.

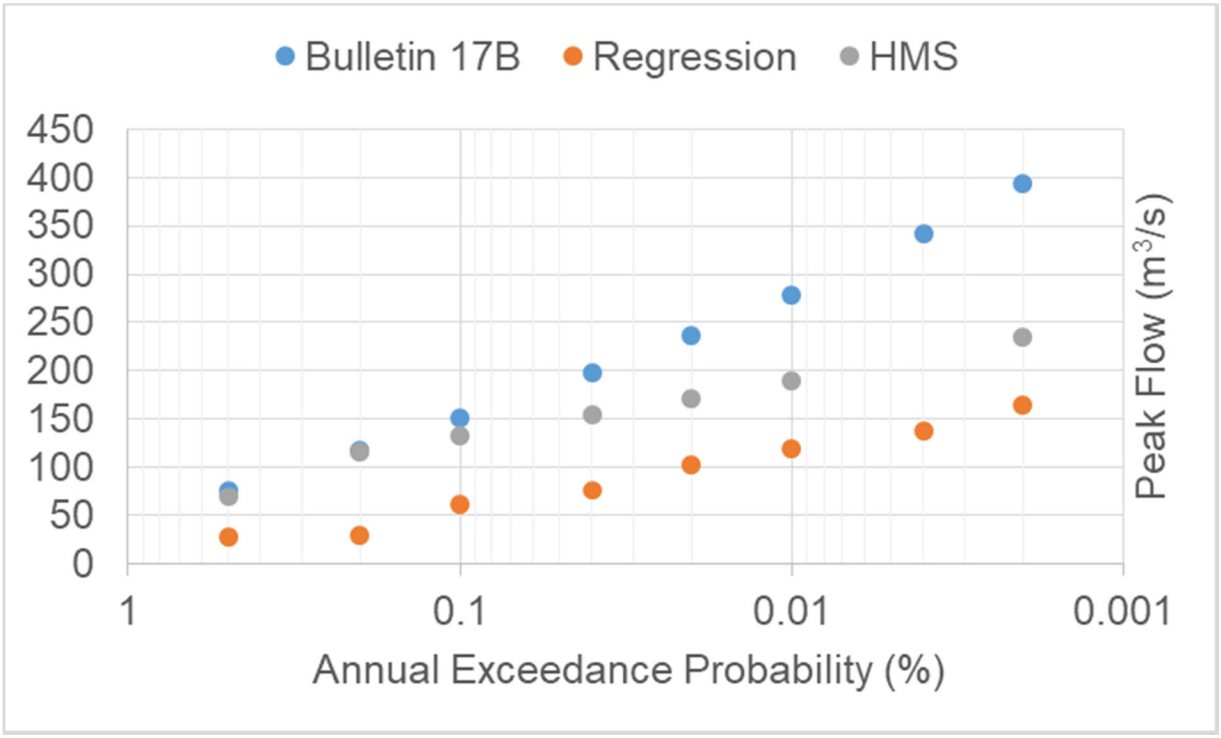

Figure 4-5: Comparison of Peak Flows at USGS 6000 Using Various Methods

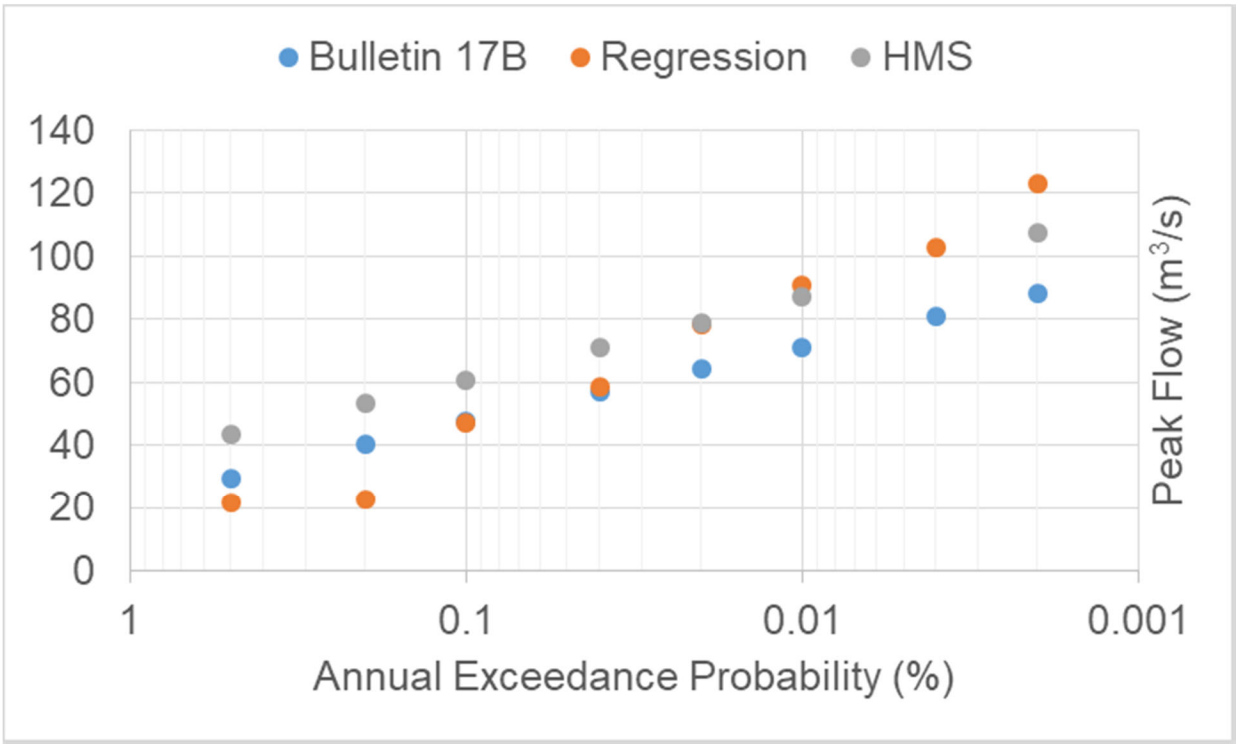

Figure 4-6: Comparison of Peak Flows at USGS 9600 Using Various Methods

5. Development of the Hydraulic Model

The hydraulic model was created using the Hydrologic Engineering Center's River Analysis System (HEC-RAS) software (version 5.0.5, HEC, 2018). The peak flow values determined in Section 4, Hydrologic Analysis were used to represent the amount of water entering the system. Field measurements and observations made during the October 2018 site visit were incorporated into the geometry of the HEC-RAS model. As a result of these efforts, a summary of flood impacts to the site are provided at the end of this section.

5.1 Flow Data

As the Umatac HMS model used site-specific information and was calibrated to historical data, the peak flows computed by the model (Table 4-22) are the most reliable and were used as the flow input for the HEC-RAS model.

5.1.1 Boundary Conditions

"Normal Depth" was the selected upstream boundary condition as flow was considered to be uniform (the slope is not very steep at the upstream boundary). The upstream slope used for normal depth computation was 0.016 for Laelae River and 0.011 for Madog River.

"Known W.S" was the selected downstream boundary condition. The mean higher high water (MHHW) from NOAA tidal stations 1630000 Apra Harbor, Guam was used as the known water surface (Known W.S) representing the downstream boundary condition. The MHHW above MSL (as the terrain data is in m above MSL) at this station is 0.26 m above MSL (or 0.85 ft MSL) (National Oceanic and Atmospheric Administration, 2017).

5.2 **Geometry Data**

5.2.1 **Reaches**

Three reaches were included in the HEC-RAS model representing the Laelae River, Madog River, and Umatac River (Figure 5-1). The Laelae River in the north and the Madog River in the south merge to create the Umatac River. In the HEC-RAS model, the Umatac River extends from the ocean outlet to a junction approximately 470 m upstream. From this junction, approximately 704 m of the Laelae River and 1,104 m of the Madog River were included in the model.

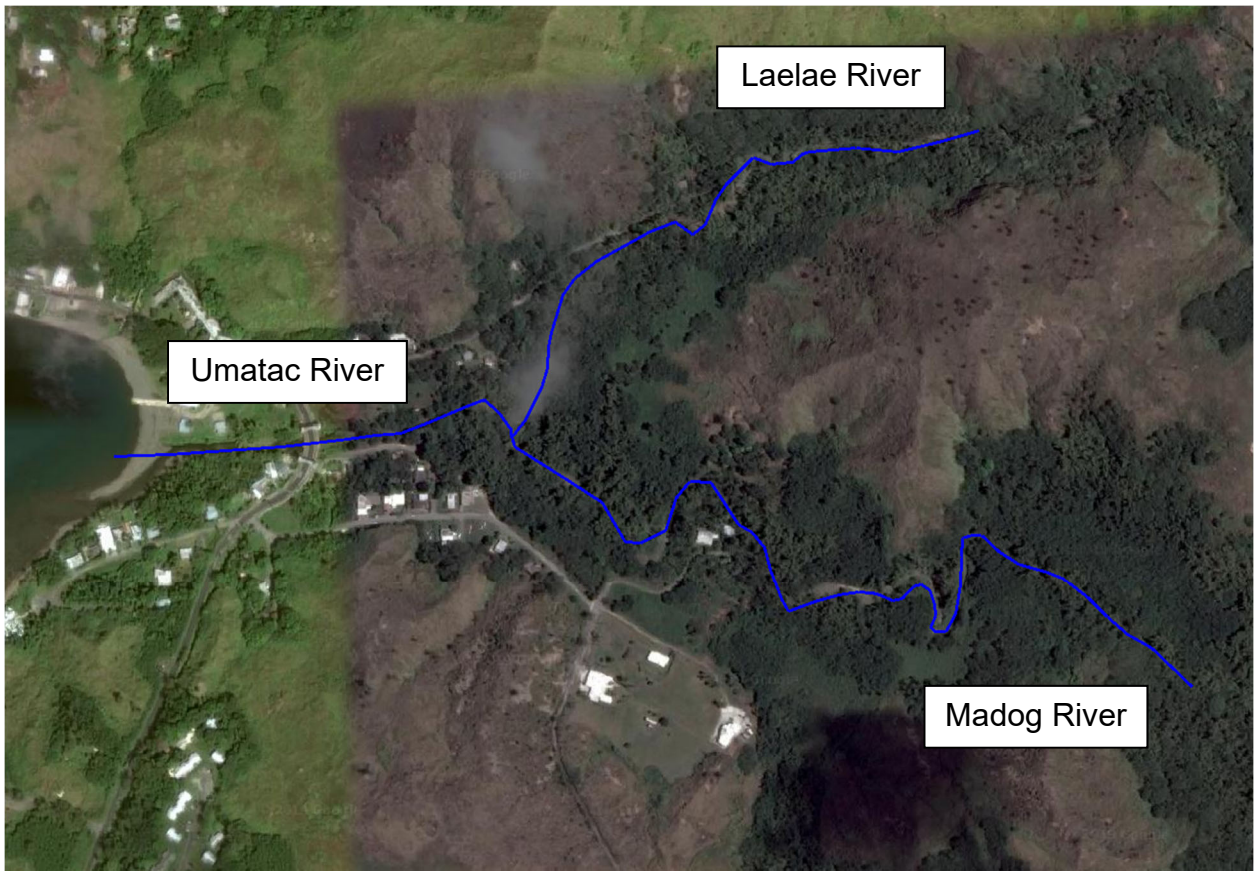

Figure 5-1: Delineated Rivers in HEC-RAS, Umatac

5.2.2 **Cross-Sections**

Cross-sections were drawn at varying intervals along the river to characterize the flow carrying capability of the river and its adjacent floodplain (see Figure 5-2). A terrain was created in HEC-RAS based on the Light Detection and Ranging (LiDAR) data collected in 2007. Initial elevations for each cross-section were extracted from this terrain and then

adjusted, as needed, to reflect measurements taken in the field during the October 2018 site visit. Such measurements include typical channel dimensions as previously presented in Table 4-3, as well as bridge and culvert dimensions, presented in Section 5.2.3.

An average cross-section spacing of 32 meters (m) was used, which is appropriate for the Umatac River. This was determined using Samuel's equation:

$$L = \frac{0.15D}{S_o}$$

where, L: Spacing of cross sections (m)

D: Bankfull depth (m)

S_o: Mean Channel Slope (m/m)

A typical bankfull depth of 3 m and mean channel slope of 0.014 was used. At some locations, more cross-sections were needed to represent a curve in the channel, junction, or bridge. The overall geometry layout, including the layout for the cross-sections, is presented as Figure 5-2.

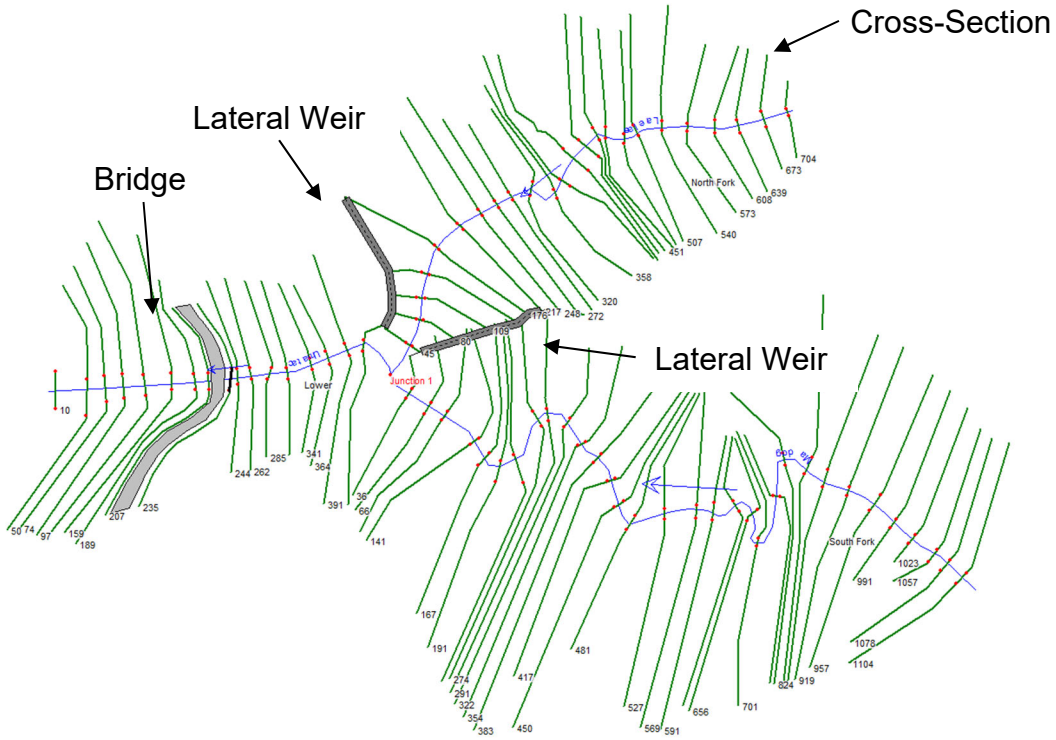

Figure 5-2: HEC-RAS Geometry Layout, Umatac

5.2.3 **Bridges**

One bridge was included in the model where Route 2 crosses the Umatac River at HEC-RAS cross-section (XS) 220 (reference Figure 5-2 and Photo 5-1).

Photo 5-1: Bridge over Umatac River at XS 220

Bridge data, as measured in the field during the October 2018 site visit, is presented in Table 5-1 and Figure 5-3. It was also noted that shoaling had caused the vertical opening in the bridge (rise) to be reduced from 2.59 m (8.5 ft) to 2.13 m (7 ft) upstream and 1.52m (5 ft) downstream.

Table 5-1: Bridge Data as Measured in the Field

River	XS	Culvert Data			Pier Width (m)	Headwall Height (m)	Deck Width (m)
		#	Span (m)	Rise (m)			
Umatac	220	1	24.4	2.59	n/a	1.83	16.6

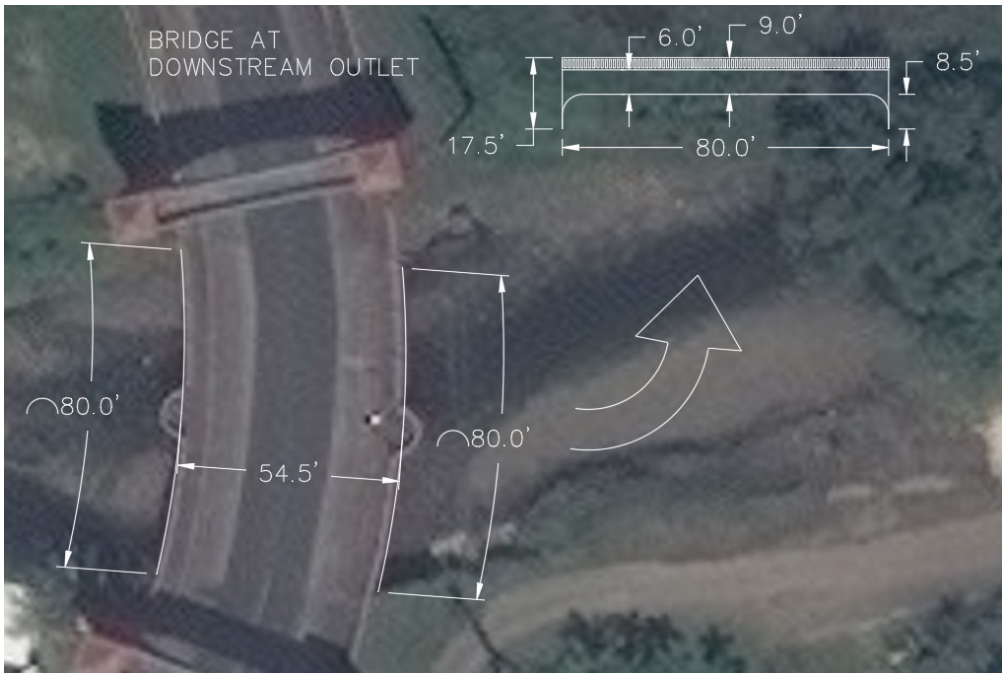

Figure 5-3: Bridge Dimensions, Umatac River as Measured in October 2018 (units in feet)

5.2.4 **Ineffective Flow Areas**

Ineffective flow areas are used to model areas which do not actively convey flow downstream, such as locations where water ponds due to the natural terrain, where water backs up into a tributary channel, or around bridges and obstructions. Ineffective flow areas were identified upstream and downstream of the Umatac Bridge. A contraction ratio of 1:1 and expansion ratio of 2:1 were used to define these areas in HEC-RAS.

5.2.5 **Lateral Weirs**

Lateral weirs are sometimes created in HEC-RAS to represent flow that crosses laterally from one river to another. Two lateral weirs were created to represent flow that may cross between the Laelae River and Madog River; and the Laelae River and Umatac River (reference Figure 5-2). A weir coefficient of 0.28 was used to represent flow over a non-elevated overbank (Goodell, 2013).

5.2.6 **Manning's n**

In the HEC-RAS model, a Manning's *n* of 0.04 was selected to represent the natural channel. Overbank areas were represented by four types of land cover: evergreen forest (0.16), forested wetland (0.12), grassland (0.035), and developed open spaces (0.04).

5.3 **Results**

The narrow channel, short overbanks, and structural constrictions along both the principal and tributary rivers result in floodwaters entering the overbank areas and residential properties as frequently as the 50% AEP (2-yr) event. The inundation map generated by the HEC-RAS model for the 1% AEP (100-yr) event is presented in Appendix A.

Based on typical sediment levels observed during the October 2018 site visit, the Umatac Bridge would be able to pass the 50% AEP (2 year) flood event with marginal flooding upstream and downstream to residential properties. During the 20% AEP (5 year) event, residential properties upstream and downstream of the bridge would begin flooding a reasonable amount. The bridge itself would overtop during the 1% AEP (100 year) event.

6. Flood Mitigation Alternatives

6.1 Reforestation

Frequent fires in the watershed have resulted in the native ravine forest being replaced with the more resilient and fire-adapted savannah grass. The impacts to the hydrology are summarized in this section with consideration toward re-establishment of the native vegetation as a potential flood mitigation alternative.

To begin, the runoff curve number (CN) for ravine forest and savannah grass are actually quite similar (55 and 58, respectively, on a scale of 0 to 100) (Natural Resources Conservation Service, 1986). ^{CN} is an empirical parameter used in hydrology to characterize the runoff properties for a particular soil and ground cover. When comparing impacts to peak flow between savannah grass and ravine forest in a single instant or storm event, there is only a very mild increase when the cover is primarily savannah grass (Roose, 1996). Bare soil, however, has a CN of 86 and would likely increase the peak flow and flood risk to the community significantly.

Savannah grass burns easily, but the roots remain alive and soon after an area burns over it sprouts again (Falanruw, 1976). Although the risk of fire and resulting bare soil is higher with savannah grass, its ability to quickly recover limits the time the soil is exposed. Small trees are often killed entirely when burned. In the short term, the savannah grass may be helping to reduce overland flow and sediment runoff by providing immediate cover to otherwise bare soil.

However, with each fire, the organic component of the soil is eroded and the ability for any type of vegetation to maintain its existence is lost, resulting in “badland” areas of bare soil. Even the savannah grasses would be unable to grow in these badland areas. Long term effects from burning and the creation of badlands are a real threat in terms of flood risk.

Other considerations that currently remain unanswered include the effectiveness of forested areas to limit the spread of fire and typical recovery times for re-establishment. Fires would likely spread more easily across dry savannah grass and burn a larger area.

For costing purposes, the reforested site was assumed to be adjacent to a main road, such as Route 2 or Jose Q. Aguon St, and planted with dominant tree species found in

the local ravine forest already: hibiscus tiliaceaus, pandanus tectorius, pandanus dubius, ficus prolixa, glochidion marriannensis, and premna serratifolia (Liu & Fischer, 2006). The estimated cost of construction to reforest a 1 acre site is approximately $51,400 with a 43% contingency for a total estimated construction contract cost of $73,600.

6.2 **Pre-Storm Cleaning**

The Umatac Bridge was modeled based on typical sediment levels observed during the October 2018 site visit (approximately 40% obstructed). Based on these sediment levels, the Umatac Bridge passes the 50% AEP (2 year) flood event with marginal flooding to residential properties upstream and downstream of the bridge; moderate to significant flooding of these residential properties would occur during the 20% AEP (5 year) event; and the bridge itself overtops during the 1% AEP (100 year) event.

Regular maintenance to remove the sediment shoals under and near the Umatac Bridge (see Photo 6-1) would increase the channel's ability to convey flood waters and reduce the bridge's risk of overtopping during a large storm event. When the amount of obstruction under the Umatac Bridge is increased to approximately 50%, the bridge overtops as early as the 10% AEP (10 year) flood event according to the simulated model. When the amount of obstruction under the Umatac Bridge is decreased to approximately 20%, the bridge overtops for events larger than the 0.2% AEP (500 year) flood event. Although the risk of overtopping is reduced in this scenario, reasonable flooding to the residential properties near the bridge still occur during the 20% AEP (5 year) event. Pre-storm clearing of the shoal near the outlet at Umatac Bay (see Photo 6-2) would also be somewhat effective in increasing the channel's ability to convey flood waters effectively.

For costing purposes, the amount of material that would be removed is approximately 500 m^3 near the bridge and 850 m^3 near the outlet. This assumes a 20% reduction of sediment under the bridge and moderate excavation of the shoal near the outlet. The estimated cost of construction is $49,800 with a 26% contingency for a total estimated construction contract cost of $62,700.

Photo 6-1: Shoal downstream of Umatac Bridge

Photo 6-2: Shoal at Umatac River Outlet, Umatac Bay

6.3 **Inline Weir and Detention Basin**

An inline weir and detention basin can be effective in reducing peak flow along a river by storing excess runoff and gradually reducing it over time. As the Madog River has a peak flow that is approximately 1.5 times greater than the Laelae River, the proposed detention basin was located along the Madog River, upstream of the developed area, and at a natural constriction in the topography (see Figure 6-1). Additionally, this feature has the added benefit of reducing the amount of sediment being transported to the ocean; however, it may also require regular removal of the sediment collected in the basin every 1-2 years.

Figure 6-1: Location of Proposed Detention Basin, Madog River, Umatac

For costing purposes, the inline weir shall be constructed similarly to the inline weir at the Namo River Flood Control Project (see Photo 6-3), with the detention basin upstream of it. The proposed dimensions of the basin are a bottom width of 18 m, side slopes of 3 horizontal to 1 vertical (3H:1V), depth of 3 meters, and length of 130 m. The

approximate cut volume total is 4,030 m^3, the approximate fill volume total is 2,680 m^3. The estimated cost of construction for the inline weir and detention basin is approximately $920,000 with a 35% contingency for a total estimated construction contract cost of $1,245,000

Photo 6-3: Inline Weir at Namo River FCP, Santa Rita, Guam

7. References

Falanruw, M. C. (1976). Life On Guam - Savanna, Old Fields, Roadsides. Territory of Guam: U.S. Office of Education - Department of Health, Education and Welfare. Retrieved from https://cnas-re.uog.edu/wp-content/uploads/2016/03/Life-on-Guam-Savanna-Old-Fields-Roadsides-2.pdf

FEMA. (2007). *Flood Insurance Study.* Federal Emergency Management Agency.

Gingerich, S. B. (2003). Hydrologic Resources of Guam. Honolulu, Hawaii, USA: U.S. Department of the Interior, U.S. Geological Survey. Retrieved from USGS Publications Warehouse: https://pubs.usgs.gov/wri/wri034126/htdocs/wrir03-4126.html

Gingerich, S. B., Keener, V., & Finucane, M. L. (2015). Climate trends and projections for Guam. Honolulu, HI, USA: East West Center. Retrieved from https://www.pacificrisa.org/wp-content/uploads/2012/01/Pacific-RISA-Guam-flyer.pdf

Goodell, C. (2013, December 24). Lateral Structure Coefficients. Davis, CA, USA. Retrieved from http://hecrasmodel.blogspot.com/2013/12/lateral-structure-coefficients.html

Google Earth. (n.d.). Map of Guam. Retrieved from earth.google.com/web/

Heitz, L. F., & Khosrowpanah, S. (2015). *Prediction of Flow Duration Curves at Ungaged Sites in Guam.* Mangilao, Guam: Water and Environmental Research Institute of the Western Pacific. Retrieved from https://guamhydrologicsurvey.uog.edu/

Interagency Advisory Committee on Water Data. (1982). *Bulletin #17B of the Hydrology Subcommittee.* Reston, VA: US Department of the Interior, Geological Survey, Office of Water Data Coordination. Retrieved from https://water.usgs.gov/osw/bulletin17B/dl_flow.pdf

Kottermair, M. (2012). *Piti-Asan Watershed Management Plan.* Mangilao, Guam: Water and Environmental Research Institute of the Western Pacific, University of Guam. Retrieved from http://www.weriguam.org/docs/reports/138.pdf

Lander, M. A., & Guard, C. P. (June 2003). *Creation of a 50-Year Rainfall Database, Annual Rainfall Climatology, and Annual Rainfall Distribution Map for Guam.* Technical Report No. 102. Mangilao, Guam: Water and Environmental Research Institute of the Western Pacific, University of Guam. Retrieved from http://www.weriguam.org/docs/reports/102.pdf

Liu, Z., & Fischer, L. (2006). Guam Vegetation Mapping Using Very High Spatial Resolution Imagery. McClellan, CA, USA: United States Department of Agriculture, U.S. Forest Service. Retrieved from U.S. Forest Service: https://www.fs.usda.gov/Internet/FSE_DOCUMENTS/fsbdev3_046054.pdf

Moriasi, D. N., Arnold, J. G., Van Liew, M. W., Bingner, R. L., Harmel, R. D., & Veith, T. L. (2007). Model Evaluation Guidelines for Systematic Quantification of Accuracy in Watershed Simulations. *Transactions of the ASABE, 50(3): 885-900*. American Society of Agricultural and Biological Engineers. doi:0001-2351

National Oceanic and Atmospheric Administration. (2017, June 20). Datums for 1630000, Apra Harbor, Guam. Apra Harbor, Territory of Guam, USA. Retrieved from https://tidesandcurrents.noaa.gov/datums.html?id=1630000

National Weather Service. (2017, April 21). NOAA Atlas 14 Point Precipitation Frequency Estimates. Silver Spring, MD, USA: US Department of Commerce, National Oceanic and Atmospheric Administration, National Weather Service. Retrieved from https://hdsc.nws.noaa.gov/hdsc/pfds/pfds_map_pi.html

National Weather Service. (2017, April 21). *NOAA ATLAS 14 POINT PRECIPITATION FREQUENCY ESTIMATES*. Retrieved from Hydrometeorological Design Studies Center Precipitation Frequency Data Server (PFDS): https://hdsc.nws.noaa.gov/hdsc/pfds/pfds_map_pi.html

Natural Resources Conservation Service. (1986). Urban Hydrology for Small Watersheds, TR-55. United States Department of Agriculture, Natural Resources Conservation Service. Retrieved from https://www.nrcs.usda.gov/Internet/FSE_DOCUMENTS/stelprdb1044171.pdf

NOAA. (n.d.). *Datums for 1630000, Apra Harbor, Guam*. Retrieved from Tides & Currents: https://tidesandcurrents.noaa.gov/datums.html?id=1630000

Roose, E. (1996). Land husbandry - Components and strategy. Rome, Italy: Food and Agriculture Organization of the United Nations, Soil Resources Management and Conservation Service Land and Water Development Division. Retrieved from http://www.fao.org/docrep/t1765e/t1765e0h.htm

Soil Conservation Service. (1985). Soil Survey of Territory of Guam. Territory of Guam, USA: United States Department of Agriculture, Soil Conservation Service. Retrieved from https://www.nrcs.usda.gov/Internet/FSE_MANUSCRIPTS/pacific_basin/PB640/0/guam.pdf

Stark, J. T. (1963). Petrology of the Volcanic Rocks of Guam. United States Government Printing Office, Washington, USA: United States Department of the Interior, Geological Survey. Retrieved from https://pubs.usgs.gov/pp/0403c/report.pdf

University of Guam. (2016, February 16). *Soils of Guam*. (USDA Natural Resources Conservation Service) Retrieved from Research & Extension: https://cnas-re.uog.edu/soils-of-guam/?where-found%5B%5D=Merizo&soil-name%5B%5D=Inarajan+series&wpv_aux_current_post_id=3244&wpv_view_count=3243-TCPID3244

USACE. (1980). *Flooding and Drainage on Guam.* Fort Shafter, HI: United States Army Corps of Engineers, Honolulu District.

USACE. (1982). *Alternative Solutions for Flood Prone Areas in Guam.* Fort Shafter, HI: US Army Corps of Engineers, Pacific Ocean Division.

USACE. (1983). *Alternative Solutions for Flood Prone Areas in Guam.* Fort Shafter, HI: US Army Corps of Engineers, Honolulu District.

USGS. (n.d.). *USGS Surface-Water Data for the Nation*. (US Department of the Interior, US Geological Survey) Retrieved from National Water Information System: Web Interface: https://nwis.waterdata.usgs.gov/nwis/sw

WERI and IREI. (n.d.). *Digital Atlas of Southern Guam*. Retrieved from HydroGuam.net: http://south.hydroguam.net/

Wong, M. F. (2010). Guam Flood Frequency Regional Regression Equations. US Army Corps of Engineers, Honolulu District.